# Characterization of the Vascular Network in a Normal Human Fundus Retina

J. Silvano Mendoza Mendiola[1], Edgardo M. Felipe Riverón[2], Flavio A. Sánchez Garfías[1], Erick Morales Silva[1], Jorge I. Ruiz Ramírez[1], y David Silva Leyva[1]

[1] Superior School for Computing, National Polytechnic Institute,
jsmendoza@ipn.mx

[2] Computing Research Center, National Polytechnic Institute
Juan de Dios Batiz w/n, P.O. 07738, Mexico
edgardo@cic.ipn.mx

**Abstract.** This paper describes a computer system to codify the vascular network in normal fundus retinal images. Digital Image Processing, mathematical morphology and artificial techniques were used to characterize relevant features of each sample. The code that characterizes the vascular network is created from the segmented and thinned vascular network that is present in the fundus of ophthalmoscopic retinal color images. Before coding the vascular network, created by means of cellular automata that scanned it completely according to 8-neighboors chain coding, the vascular cluster located into the optic papilla was excluded, since it has not particular advantage in the code. In order to get a code invariant to rotation, a new code is generated with the difference of successive positions of the original code. In such a form, the code is invariant to rotations when the rotation angle is multiple of 45°.

**Keywords:** Vascular Network, Retina, Image Segmentation, Mathematical Morphology, Coding.

## 1 Introduction

In medicine, criminology, and security areas the use of digital images has acquired great importance. In ophthalmology the observation and treatment of pathologies, which are reflected in patient's retinas, is very common. Nowadays, in security systems the vascular network analyses of human retinas provide a good solution to a personal biometric authentication. The work reported in this paper has been oriented to similarly provide an effective solution to the problem of characterizing the vascular network in images of normal human fundus retina.

## 2 The Human Retina

The retina is the innermost membrane of the eye, which covers approximately 60% of the rear wall of the eyeball. When the eye is properly focused, the light reflected from an object located outside the eye is imaged on the retina. Vision of objects is afforded by means of discrete light receptors distributed over the surface of the retina. There are two classes of receptors: *cones* and *rods*. The number of cones per eye is about 6 to 7 million. They are located primarily in the central portion of the retina, called the *fovea*, and are highly sensitive to color. Human beings can resolve largely fine details with these cones because each one is connected to its own nerve fiber. Cone vision is called *photopic* or bright-light vision.

The number of rods is much larger. Some 75 to 150 million are distributed over all the retinal surface. The larger area of distribution and the fact that commonly several rods are connected to a single nerve fiber the amount of detail discernible by these receptors is more limited. Rods give a general overall picture of the field of view. They are not involved in color vision and are sensitive to low levels of illumination. For example, objects that appear brightly colored in daylight when are seen in moonlight appear as colorless forms because only the rods are stimulated. This phenomenon is known as *scotopic* or dim-light vision [1].

There are three visible anatomical elements present in the fundus of the retina: the macula, the optic disk (or optic papilla), and the vascular network, composed of the thicker and darker red vein network, and the thinner arterial network of clearer reddish tones. The vascular network is the anatomic element of interest in this paper.

### 2.1 The Vascular Network

The vascular network permits the blood flow in the retina to carry out the metabolic processes that feed the retina. It covers the entire retina. Both, the arterial network and the venous network dichotomize twice to form four independent branches. In a normal retina its access from the choroids is through the center of the optic disk, which is the visible part of the tubular duct that leads the nerve fibers from the retina photosensitive elements towards the brain (Fig. 1).

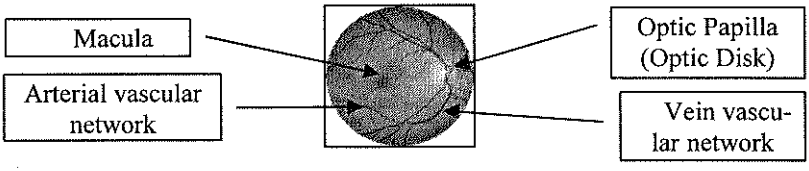


**Fig. 1.** Digital image of the fundus of a normal human retina

### 2.2 Structure of the Vascular Network

The general structure of the vascular network resembles the branches of a tree or the bed of a river. Its thickness from the optic papilla varies gradually from thick to thin as the retina branches. Along both arterial and venous networks, there are bifurcations, which cause the network to systematically extends itself in many directions. It is common that both networks interlace each other but always the arterial network remains over the venous network. Bifurcations normally take place at angles that are less than 45°, and rarely greater.

Because of the variability of the network paths, is nearly impossible for two individuals to have equal vascular networks. Networks of both eyes are also different. Thus, the structure of the network can be used as a reliable personal biometric authentication method.

## 3 The Problem and Some Antecedents

The problem is to obtain a numeric code that characterizes the paths of a vascular network in the fundus of normal retinal images. The code should be invariant to rotation and translation of the original image.

In our application, the code is obtained from all the visible parts of the fundus, although in actual systems used for identification the code could be from the upper and/or lower venous and arterial temporal branches because they are the more clearly visible in the captured images.

Images used are ophthalmoscopic color images, preferably taken with a non-midriatic eye fundus camera with an opening angle of 45°. In our case we used a midriatic camera, which requires that the pupil be previously dilated.

Some algorithms have been developed to identify and characterize vascular networks of the fundus of the retina. Amongst them, some use linear and non-linear filtering [8], morphological methods [2, 8], neural networks, and algorithms that quantify sections of the vascular network. An algorithm developed recently in France uses mathematical morphology to segment the vascular network. It uses four fundamental steps: noise cleaning, enhancing of linear patterns using a Gaussian profile, evaluation of the curvature, and linear filtering [3]. The algorithm has been used on eye fundus images to diagnose hypertension and diabetes.

## 4 General Sequence of the Characterization Process

The general sequence of operations proposed in this paper to characterize the vascular network is:

1. Capture of the ophthalmoscopic RGB color image.
2. Select the image in the green plane.
3. Transform this image into gray scale.
4. Segment and enhance the vascular network in the eye fundus.
5. Thin the vascular network.
6. Exclude the vascular cluster inside the papilla.
7. Generate the numerical code of the segmented vascular network.

## 5 Morphological Operators

egmentation of the vascular network was carried out using morphological operators. A short summary of the operators for gray levels images used in this paper is given next [4]. More details about these would be found in [1].

We define a two-dimensional (2-D) digital image with a gray level range $[N_{min}, N_{max}]$, as a function $\boldsymbol{S} : \Re^2 \rightarrow [N_{min}, N_{max}]$, and a 2D structuring element as a function $\boldsymbol{B} : \Re^2 \rightarrow \boldsymbol{B}$.

Erosion:

$$(f \Theta g)(x, y) = \min\{f(x+s, y+t) - g(s,t) : (x+s, y+t) \in Dom(f), (s,t) \in Dom(g)\} \quad (1)$$

Dilation:

$$(f \oplus g)(x, y) = \max\{f(x-s, y-t) + g(s,t) : (x-s, y-t) \in Dom(f), (s,t) \in Dom(g)\} \quad (2)$$

Opening:

$$A \circ B = (A \Theta B) \oplus B \quad (3)$$

Closing:

$$A \bullet B = [A \oplus (-B)] \Theta (-B) \quad (4)$$

Top Detector (Top-Hat)

$$TOPHAT(f) = f - (f \circ g) \quad (5)$$

Valleys Detector (Bot-Hat)

$$BOTHAT(f) = (f \bullet g) - f \quad (6)$$

Elemental Geodesic Dilation:

$$\delta^{(1)}{}_I(J)=(J\oplus B)\cap I \tag{7}$$

Elemental Geodesic Erosion:

$$\varepsilon^{(1)}{}_I(J)=(J\ominus B)\cup I \tag{8}$$

Reconstruction by Geodesic Dilation:

$$P_I(J)=\bigcup_{n\geq 1}\delta^{(n)}{}_I(J) \tag{9}$$

Reconstruction by Geodesic Erosion:

$$P^*{}_I(J)=\bigcap_{n\geq 1}\varepsilon^{(n)}{}_I(J) \tag{10}$$

## 6 Description of the System

Next we present a short description of the procedures used for characterizing the vascular network of the fundus in normal ophthalmoscopic color images of the human retina.

### 6.1 Capture and Preprocessing of the Image

Figure 2 shows the green plane of a typical color ophthalmoscopic digital image. The only requirement for capturing these images is that the pupil be dilated. The Interdisciplinary Center of Health Sciences (CICS) of the National Polytechnic Institute and the ophthalmologists Dr. Antonio Lopez Bolaños and Dr. Sandra Ortiz Yáñez gave us the images used in this work. Images were captured with a color photographic digital camera matched to a midriatic eye-fundus camera. They have been normalized in size to 360 x 288 pixels; they are in BMP format ("bitmap") with a total intensity resolution of 24 bits/pixel. The vascular network thickness in the thickest part is 9 pixels.

The color model used is RGB. From the three color channels we selected the green channel because in the visible zone of the electromagnetic spectrum, the green color is located in the center, that is why it is prone to contain less additive noise (Fig. 2).

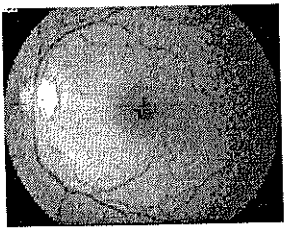

**Fig. 2.** Image from the green plane

### 6.2 Segmentation of the Vascular Network

The first task in the characterization process was the separation of the vascular network from the other structural elements present in the retinal image. This was accomplished using the *Maximum of Openings* defined by Zana and Klein [2] and by Flynn [3] (Eq. 11). This technique reduces background noise and preserves the blood vessels.

$$I_C = \max_{i=1..16}\{I_0 \circ B_i\} \tag{11}$$

where $I_C$ is the resultant image, $I_0$ is the original image, and $B_i$ is the structuring element rotated 16 times.

We used a linear flat structuring element of height 0 and 9 pixels of length, rotated 16 times, in order to obtain a background nearly uniform and smooth image gray levels.

Then we used a *Sum of Valleys* also defined by Zana and Klein [2] and by Flynn [3]:

$$I_{SUM} = \sum_{i=1}^{16} BOTHAT(I_C, B_i) \tag{12}$$

where $I_{SUM}$ is the resultant image, $I_C$ is the original image and $B_i$ is a structuring element rotated 16 times.

We used the same set of structuring elements, as in the last step, to obtain only the protuberances of our network, as shown in the Fig. 3.

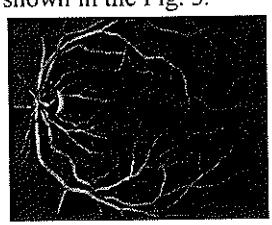

**Fig. 3.** Resultant image after the Maximum of Openings and then the Sum of Valleys with a plane structuring element with height 0 and 9 pixels length, rotated 16 times

Another Maximum of Openings was applied to the resultant image with the same set of structuring elements in order to isolate the vascular network from the non-uniform background.

Next we made a Reconstruction by Geodesic Dilation using a circular structuring element (disc), with height 0 and 5 pixels length. The two threshold levels used in the reconstruction were automatically obtained from histogram values according to the first two minima found (Fig. 4). Each image has a different histogram, so we have to examine the histogram of each image to find the two optimal thresholds levels. The first threshold is for obtaining the mask image, and the second is for the marker image required by the

reconstruction. Figure 4b shows the vascular network reconstructed with thresholds values of 8 and 15 obtained from the histogram.

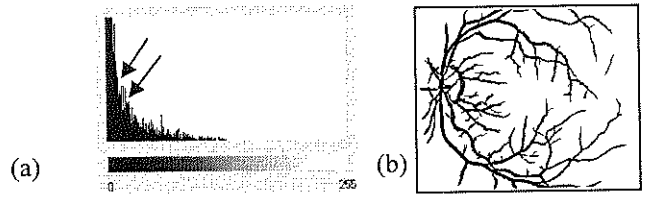


**Fig. 4.** (a) Histogram used to obtain the optimal threshold levels, in this case 8 and 15. (b) Segmented vascular network after the morphological operations

### 6.3 Vascular network thinning

From the segmented image, we used the Zhang-Suen algorithm for thinning [5], eliminating the redundant pixels according to Sossa [6]. This solution creates a path with a thickness of a pixel, but maintains the connectivity in the neighborhood and never breaks the line. Afterwards we made a Sossa [6] post processing to improve the results obtained with the algorithm of Zhang-Suen [5] as proposed in [7] (Fig. 5).

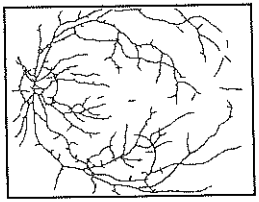

**Fig. 5.** Vascular network thinned with Zhang-Suen algorithm and corrected with pos processing from Sossa

### 6.4 Segmenting the Optic Disk

The vascular network permits the blood flow in the retina to carry out the metabolic processes that feed the retina. Then, it spreads around the entire retina. The arterial network that leads the blood to the retina dichotomizes in order to create the upper and lower branch arteries, and each of its branches is dichotomized again to create the nasal branch and the temporal branch.. Access in a normal retina from the choroids is through the center of the optic disk, which is the visible part of the tubular duct that leads the nerve fibers from the retina photosensitive elements towards the brain. This confluence of veins and arteries conform a vascular bunch in the papilla, from which it is very difficult to define the paths (Fig. 1). So, in our work networks located into the papilla zone are

covered in images by an opaque circular patch. For this reason we have to detect the position of the papilla exactly.

For the types of images used in this work, the optic disk has an approximate diameter of 60 pixels. To segment the optic disk, we start the search up from the threshold level 127, we look for the first minimum in the green channel histogram, and use this value to generate a binary image. To the resultant image we apply a morphological dilation with a disk-shaped structuring element of 30 pixels in diameter and a height of 0. In this way, we obtain a binary image with the certainty that the image is centered in the optic disk (Fig. 6b). Next the position of the centroide is calculated by tracing a circle over the vascular thinned image (Fig. 7).

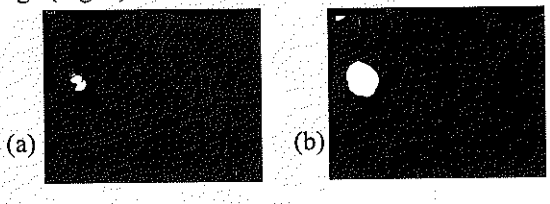


**Fig. 6.** (a) Thresholding of the image in level 131. (b) Image after dilation with a circular structuring element with a diameter of 30 and a height of 0

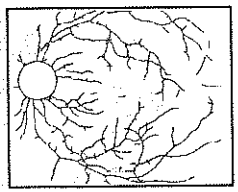

**Fig. 7.** Vascular network with optic disk occluded using an opaque disk, already for coding

## 7 Coding

When the optic disk is hidden to avoid ambiguities due to the vascular bunch, its periphery is used as the origin of all the network branches to obtain a code that characterizes it. To describe the paths of the vascular network we used cellular automata. Coding was done following the 8-directions pattern shown in Fig. 8a, and the 3 x 3 neighbor mask shown in Fig. 8b.

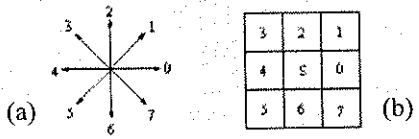


**Fig. 8.** (a) Chain code with 8-neighbors. (b) 3 x 3 mask to create the chain code

Each automaton starts from the circumference occluding the optic disk and for each branch a new automaton is created. When the automaton goes ahead, pixels are marked as visited. The code is stored in a text file. To create the code, the following convention was used:

Letter "i" indicates the beginning of the branch to be coded. Two asterisks indicate that a two-child automaton has been created due to a bifurcation.

Now it is necessary to create the code that describes the structure of the network. For this, a 3 x 3 pixels mask was used (Fig. 8b), which assigns a code according to the pixel position following the 8-neighbor pattern, with the current pixel at its center S.

When the automaton finds a bifurcation, the parent automaton creates two child automata. Figure 9 illustrates the concept, where a small sample of the code is shown. After this, we continue the description, with each child followed by a carriage return.

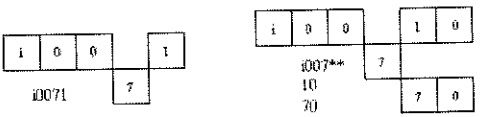

**Fig. 9.** Examples of paths in one-pixel vascular network, a bifurcation, and corresponding codes.

In order to determine its current direction, each automaton verifies the "last step code", that is, all automata verify the last code created in the way. For this, the mask in Fig. 10 was used.

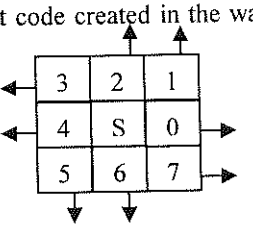


**Fig. 10.** Mask used to obtain the orientation of automata

When all pixels of the vascular network have been visited, the next phase is to eliminate discontinuities by connecting the ends that are located less than 12 pixels away from the current pixel. To carry out this process with high reliability, an analysis window of 12 x 12 pixels was used. When an automaton finds such point, it joins the last coded pixel with the new point located inside the analysis window. From the final code obtained to characterize the vascular network, it was reconstructed again to verify its effectiveness.

## 8 Results

Figure 11 shows several images with the vascular network segmented, thinned to one-pixel width, and the optic disk occluded. An example of the code is shown in Fig. 9.

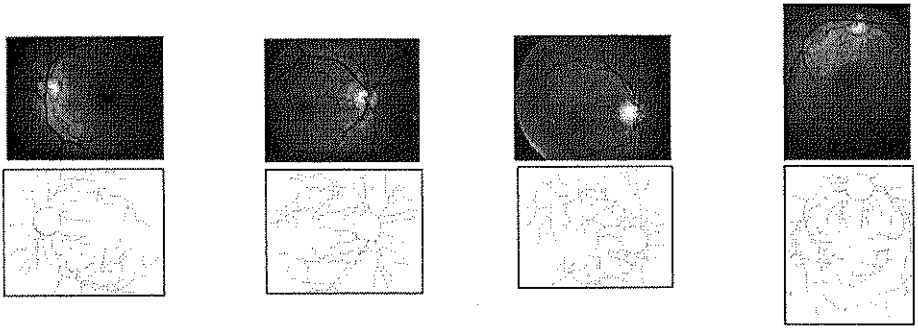

**Fig. 11.** Five original images with the vascular network segmented, thinned to one-pixel width and their optic disk occluded

## 9 Limitations of the Code

In order to get a code invariant to rotation, a new code is generated with the difference of successive positions of the original code. The image of the retina located to the right in Fig. 11 is shown rotated 90°, to test the invariance to rotation of the code of differences obtained. It was verified that the code was the same than that of the image not rotated. This always occurs when the rotation angle is multiple of 45°, which are the positions controlled by the 8-neighbor pattern used for coding. At the same time, the circle occluding the optic disk must be situated exactly at the same relative position in both images. In images rotated an angle different to a multiple of 45°, the obtained code is different to the original one, due to the position of pixels in the rotated image results with some differences with respect to the original.

## 10 Conclusion

The procedure proposed in this work characterizes with a numerical code the vascular network extracted from color ophthalmoscopic retinal images. Chain coding following the 8-neighbor pattern creates the code. For this task the segmentation of the vascular network must be of a high quality Segmentation was carried out using morphological techniques based on maximum of openings and sum of valleys, followed by a maximum of opening, with an adequate structuring elements. Morphological reconstruction enhances the segmentation by using a binary marker and mask images obtained from thresholds directly found at two consecutive minima obtained from the histogram of the original image. In order to overcome problems with a vascular bunch (or cluster) located inside the optic disk, it was occluded with an opaque disk created from the segmented image of the optic

papilla. It was verified that the code of differences calculated from the original code of the vascular network is invariant to rotation in angles multiple of 45°. A logical extension of this work is to use a 16-directional pattern with a separation angle of 22.5°, or approximating the original network with linear segments.

## References

1. Rafael C. Gonzalez, Richard E. Woods, 2002, Digital Image Processing, 2nd. Edition, Prentice Hall.
2. F. Zana and J. C. Klein, 2001, "Segmentation of Vessel-Like Patterns Using Mathematical Morphology and Curvature Evaluation" *IEEE Transactions on Image Processing*, Vol. 10, No.7, pp. 1010-1019.
3. Flynn, J, 2000, "Automated vessel extraction in digital ophthalmic images", http://www_video.eecs.berkeley.edu/~johnf/thesis.pdf .
4. J. Serra, 1982, "Image Analysis and Mathematical Morphology". London, U.K.: Academic.
5. T.Y. Zhang, C.Y. Suen, 1984, "A fast parallel algorithm for thinning digital patterns", *Communications of ACM*, Vol. 27, Num 3.
6. Juan Humberto Sossa, 1989, "An improved parallel algorithm for thinning digital patterns" *Pattern Recognition Letters*, Vol. 10.
7. Juan Luis Díaz de León Santiago, 1991, "Algoritmos de esqueletización de imágenes digitales binarias", CINVESTAV –IPN.
8. F. Zana and J. C. Klein, 1999, "A Multimodal Registration Algorithm of Eye Fundus Images Using Vessels Detection and Hough Transform", IEEE *Transactions on Medical Imaging*, Vol. 18, Num. 5.